

## RESEARCH ARTICLE

DNA damage induces Yap5-dependent transcription of *ECO1/CTF7* in *Saccharomyces cerevisiae*Michael G. Mfarej, Robert V. Skibbens<sup>1</sup>\*

Department of Biological Sciences, Lehigh University, Bethlehem, Pennsylvania, United States of America

\* [rvs3@lehigh.edu](mailto:rvs3@lehigh.edu)

## OPEN ACCESS

**Citation:** Mfarej MG, Skibbens RV (2020) DNA damage induces Yap5-dependent transcription of *ECO1/CTF7* in *Saccharomyces cerevisiae*. PLoS ONE 15(12): e0242968. <https://doi.org/10.1371/journal.pone.0242968>

**Editor:** Marco Muzi-Falconi, Università degli Studi di Milano, ITALY

**Received:** March 28, 2020

**Accepted:** November 12, 2020

**Published:** December 29, 2020

**Copyright:** © 2020 Mfarej, Skibbens. This is an open access article distributed under the terms of the [Creative Commons Attribution License](https://creativecommons.org/licenses/by/4.0/), which permits unrestricted use, distribution, and reproduction in any medium, provided the original author and source are credited.

**Data Availability Statement:** All relevant data are within the manuscript and its [Supporting information](#) files.

**Funding:** This work was supported by an award to R.V.S. from the National Institutes of Health [R15GM110631] and a research fellowship award to MGM. The funders had no role in the study design, data collection and analysis, decision to publish, or preparation of the manuscript.

**Competing interests:** No. The authors have declared that no competing interests exist.

## Abstract

Yeast Eco1 (ESCO2 in humans) acetyltransferase converts chromatin-bound cohesins to a DNA tethering state, thereby establishing sister chromatid cohesion. Eco1 establishes cohesion during DNA replication, after which Eco1 is targeted for degradation by SCF E3 ubiquitin ligase. SCF E3 ligase, and sequential phosphorylations that promote Eco1 ubiquitination and degradation, remain active throughout the M phase. In this way, Eco1 protein levels are high during S phase, but remain low throughout the remaining cell cycle. In response to DNA damage during M phase, however, Eco1 activity increases—providing for a new wave of cohesion establishment (termed Damage-Induced Cohesion, or DIC) which is critical for efficient DNA repair. To date, little evidence exists as to the mechanism through which Eco1 activity increases during M phase in response to DNA damage. Possibilities include that either the kinases or E3 ligase, that target Eco1 for degradation, are inhibited in response to DNA damage. Our results reveal instead that the degradation machinery remains fully active during M phase, despite the presence of DNA damage. In testing alternate models through which Eco1 activity increases in response to DNA damage, the results reveal that DNA damage induces new transcription of *ECO1* and at a rate that exceeds the rate of Eco1 turnover, providing for rapid accumulation of Eco1 protein. We further show that DNA damage induction of *ECO1* transcription is in part regulated by Yap5—a stress-induced transcription factor. Given the role for mutated *ESCO2* (homolog of *ECO1*) in human birth defects, this study highlights the complex nature through which mutation of *ESCO2*, and defects in *ESCO2* regulation, may promote developmental abnormalities and contribute to various diseases including cancer.

## Introduction

In order for a cell to divide, the cell division cycle must accomplish two major feats with high fidelity. First, the genetic material must be accurately replicated during S phase. Second, the cell must segregate the duplicated genetic material to each daughter cell during M phase. To identify over time the products of chromosome duplication, the cell tethers together sister chromatids during S phase. Sister chromatid tethers, or cohesins, are comprised of a group of

conserved proteins (Smc1, Smc3, Mcd1/Sccl/Rad21) and auxiliary factors (Pds5 and Sccl/Irr1) that maintain sister identity until anaphase onset [1–4]. Cohesion establishment during S phase requires an additional essential factor, Eco1/Ctf7 (herein Eco1), that is part of the GNAT-family of N-acetyltransferases [5–7]. Eco1 acetylates the Smc3 subunit of cohesin, converting chromatin-bound cohesins to a tether-competent state [7–10]. At the cellular level, mutations in *ECO1* result in aneuploidy, reduced chromatin condensation reactions, and increased sensitivity to DNA damage [5,11–14]. In humans, mutations in *ECO1* orthologs (termed *ESCO1/EFO1* and *ESCO2/EFO2*) collectively correlate with numerous forms of cancer, including melanoma and prostate cancer, and a severe developmental abnormality called Roberts Syndrome (RBS) [15–20].

Early cell cycle mapping studies revealed that Eco1 function is required only during S phase and linked Eco1 function to the DNA replication processivity factor PCNA [5]. This link between Eco1, cohesion establishment, and DNA replication factors is now well established [3,5,6,8–10,21–31]. The mechanism through which Eco1 function is limited to S phase, however, was only recently elucidated. At the end of S phase, Eco1 is phosphorylated (S99) by the cell cycle regulator Cdk1. Eco1<sup>S99-P</sup> becomes a target for second-site phosphorylation (S98) by Dbf4-Cdc7 (DDK) kinase complex, a regulator of DNA replication initiation [32–35]. Eco1<sup>S98-P, S99-P</sup> becomes a target for third-site phosphorylation by the GSK-3 signaling kinase Mck1, which in turn phosphorylates Eco1 at S94. Eco1<sup>S98-P, S99-P, S94-P</sup> is then ubiquitinated by SCF and subsequently degraded following DNA replication [34,36]. Notably, XEco2 (Xenopus) and ESCO2 also are degraded following DNA replication [17,37,38], revealing that limiting Eco1 function to S phase is highly conserved through evolution.

Although sister chromatid tethering is typically restricted to S phase, a special form of cohesion is established during M phase in response to a double strand break (DSB)—an activity termed damage-induced cohesion (DIC) [12,13,39,40]. Beyond occurring in different cell cycle phases, cohesion and DIC differ in two important aspects. First, acetylation of Smc3 is not sufficient to generate cohesion during DIC, as opposed to S phase cohesion [41,42]. Instead, DNA damage induces Mec1, a DNA damage signaling kinase, to phosphorylate Mcd1 at S83 [41]. Phosphorylated Mcd1 recruits Eco1 which in turn acetylates Mcd1 at K84 and K210, resulting in DIC [42]. Loss of Mcd1 acetylation abolishes DIC and inhibits homologous recombination (HR)-based DNA repair, linking defects in DIC to mutagenic forms of DNA repair such as non-homologous end-joining [12,13,39,40,42]. Thus, mutation of *ESCO2*, or defects in pathways through which DIC becomes activated in response to DNA damage, likely play an important role in human development. Second, Eco1 establishes cohesion at both sites of DNA damage and along undamaged chromosomes in response to DSB. Thus, DIC occurs independent of DNA repair fork components, in contrast to S phase cohesion which occurs through recruitment of Eco1 to the DNA replication fork by PCNA [5,12,13,23,31].

Given that Eco1 is degraded during late S, how is DIC established during M phase? Notably, overexpression of Eco1 in M can drive a second round of cohesion in the absence of DNA damage [42]. This suggests that DNA damage may stabilize Eco1 protein to promote DIC during M phase. Based on elegant biochemical studies that document sequential phosphorylation leading to Eco1 ubiquitination and degradation, one plausible model of Eco1 stabilization during M phase is that Eco1 phosphorylation is inhibited, blocking subsequent ubiquitination and degradation [34–36,43–45]. A second mode of Eco1 stabilization might include directly reducing SCF ubiquitination activity and/or proteasome degradation. Here, we test these models. The results reveal that the degradation machinery is fully operational during DIC, but that elevated rates of Eco1 transcription outpace Eco1 degradation. We further report that this transcription relies in part on Yap5—a transcription factor currently implicated in stress responses [46–48]. Our results revise current models of Eco1 regulation.

## Materials & methods

### Yeast strains

*Saccharomyces cerevisiae* strains used in this study are listed in [Table 1](#).

### General methods

Log phase cultures were maintained at 23°C and normalized to an OD<sub>600</sub> = 0.2–0.4 in all experiments. G<sub>1</sub> and S phase arrests in cell cycle time course experiments were achieved by incubating cells in YPD supplemented with Alpha Factor and hydroxyurea (HU; 200mM final concentration) for 3 hours at 23°C, respectively. Alpha Factor and HU was washed out and the cells rinsed with YPD followed by incubation in fresh YPD supplemented with nocodazole (20<sup>µg</sup>/mL) at 23°C for the indicated time periods. Assessment of DNA content by flow cytometry were performed as previously described [26]. Translation inhibition was achieved by addition of 100<sup>µg</sup>/mL cycloheximide (Sigma) at 23°C for the indicated time points. DNA damage induction was achieved by addition of 0.1% MMS (Sigma); 333<sup>µg</sup>/mL Zeocin (Invitrogen) or 200mM HU (Sigma) for the indicated time periods at 23°C.

### Western blot analysis

Whole cell extracts were made by TCA precipitation as previously described [49]. Proteins were resolved by SDS PAGE followed by transfer to PVDF membrane using the Trans-Blot Turbo Transfer System (Bio-Rad). Western blot analysis for Eco1 was performed using mouse-anti-V5 primary antibody (Invitrogen), Goat-anti-mouse HRP secondary (Bio-Rad) followed by detection with ECL Prime (GE). To assess Rad53 phosphorylation, samples of MMS-treated cells were prepared by TCA precipitation in the presence of 1% PPI3 phosphatase inhibitor (Sigma). Membranes were probed with anti-Rad53 primary antibody (Santa Cruz, yC-19 for [Fig 2C](#); Abcam, ab104232 for [Fig 2G](#) and [S2C Fig](#)) and Donkey-anti-Goat HRP/Goat-anti-Rabbit HRP secondary antibody. All images were obtained by exposing ECL treated blots onto X-ray film followed by scanning with an office scanner (EPSON Perfection V300 Photo). Western blot quantification analysis is shown to represent variation between biological replicates and was performed using ImageJ by normalizing Eco1 signal to the loading control PGK within respective lanes. Normally distributed peaks were measured using the entire area of the signal. Quantifications represent one measurement of each sample. Histograms represent quantification of the averaged amount of normalized Eco1 protein within each drug-treated sample divided by the normalized Eco1 protein level in the untreated sample.

### RNA extraction and quantitative real-time PCR

Cells were pelleted by centrifugation and immediately frozen in liquid nitrogen. RNA extraction was performed using the RNeasy Mini Kit (Qiagen) per the manufacturer's instructions. Cell lysis was performed by bead beating in buffer RLT supplemented with 10µl BME/mL.

**Table 1.**

Strain	Genotype	Reference
YBS1334	<i>MATa; ECO1-3v5:HIS3; A364A</i>	This study
YMG49	<i>MATa; lys2::KAN; BY4741</i>	<i>Saccharomyces</i> Genome Deletion Project
YMG50	<i>MATa; yap5::KAN; BY4741</i>	<i>Saccharomyces</i> Genome Deletion Project

<https://doi.org/10.1371/journal.pone.0242968.t001>

Purification of total RNA was followed by subsequent RNA clean-up using the RNeasy mini kit (Qiagen) per the manufacturer's instructions. Quantitative Real-Time (qRT) PCR was performed using the QuantiNova SYBR Green RT-PCR kit (Qiagen) and  $C_T$  values measured using the Rotor-gene (Corbett). The  $C_T$  values for *ECO1* and the internal control, the 26S proteasome subunit, *RPN2*, were averaged. The  $\Delta C_T$  values represent the expression levels of *ECO1* normalized to *RPN2* values, an established internal control for qRT-PCR [50].  $\Delta\Delta C_T$  values represent the relative level of gene expression. The fold difference was determined using the  $\Delta\Delta C_T$  method ( $2^{-\Delta\Delta C_T}$ ) as previously described [51]. Briefly, the  $\Delta C_T$  is determined by subtracting the average *RPN2*  $C_T$  from the average *ECO1*  $C_T$ . The standard deviation of the  $\Delta C_T$  is calculated from the standard deviations of the *ECO1* and *RPN2* values using the Comparative Method [52].

## Results

### Eco1 is degraded following DNA replication

Eco1-dependent establishment of sister chromatid cohesion is typically limited to S phase [5,6,9,10,24]. This model is supported by cell cycle mapping studies and compelling findings that Eco1 undergoes highly orchestrated and sequential phosphorylation modifications that target Eco1 for degradation during late S phase and through M phase [5,34–36]. Challenging this model, however, are other studies that failed to detect significant changes in Eco1 protein levels across the cell cycle [6,23]. Thus, it became important to independently assess whether Eco1 protein levels change across the cell cycle. Briefly, cells harboring Eco1-3V5, as the sole source of Eco1 protein, were synchronized in early S phase with hydroxyurea (HU), washed and then incubated for three hours in fresh media supplemented with nocodazole (NZ) to achieve an M phase arrest (Fig 1A). Cell cycle progression and Eco1 protein levels were monitored by flow cytometry and Western blot, respectively (Fig 1B and 1C). The results show that Eco1 levels are high during S phase (when cohesion is established) and then drop dramatically as cells progress into M phase (Fig 1C). To determine if Eco1 protein level reduction following HU-arrest was an artifact of stalled replication forks, cells harboring Eco1-3V5 were arrested in Alpha Factor for three hours, washed and then incubated for three hours in fresh media supplemented with NZ (S1A Fig). Cell cycle progression and Eco1 protein levels were monitored every hour following Alpha Factor release by flow cytometry and western blot, respectively (S1B and S1C Fig). The results indicate that Eco1 levels are low in G1, peak during DNA replication (S-phase) and decline in M-phase. These results, and those obtained using HU synchronization, are consistent with cell cycle mapping [5] and biochemical studies [34,36].

### DNA damage during m phase induces *de novo* synthesis of Eco1 protein

Eco1 protein levels are very low during M phase, but increase in response to genotoxic agents such as HU, 4-NQ (UV mimetic that induces thymidine dimers) or zeocin (DSB inducer) [34,36]. To independently validate that DNA damage induces an increase in Eco1 protein levels during M phase, both log phase and NZ-arrested cells were treated with 0.1% methyl methanesulfonate (MMS—a DNA alkylating agent) for 1 hr (S2A Fig). Cell cycle state and Eco1 protein levels were monitored by flow cytometry and western blot, respectively (S2B & S2C Fig). In log phase and NZ-arrested cultures, MMS-induced 1.5- and 2.8-fold increases in Eco1 protein levels, respectively, compared to cells not exposed to MMS (S2C Fig). The increase in Eco1 protein levels in both log phase and NZ-arrested cultures coincided with Rad53 phosphorylation (S2C Fig), confirming induction of the DNA damage checkpoint in response to MMS.

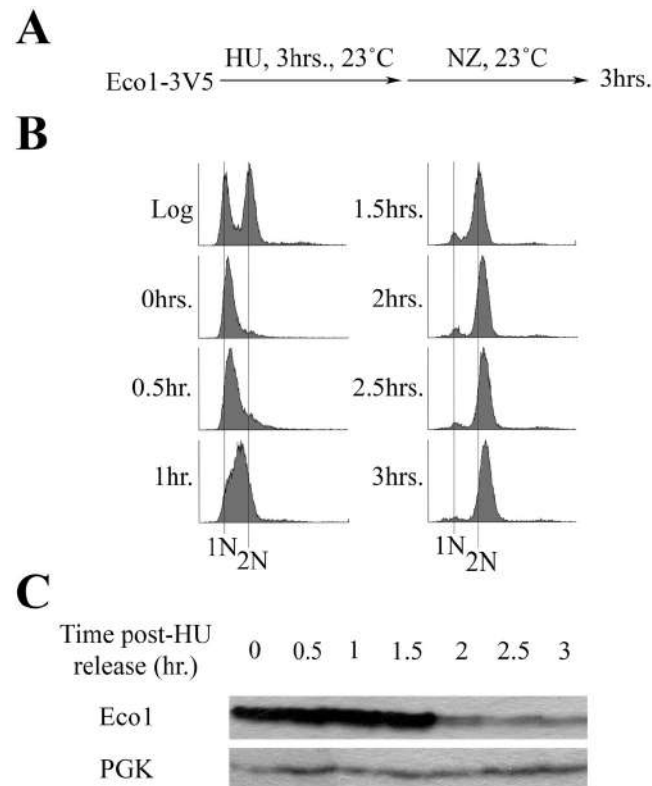


**Fig 1. Eco1 protein levels decline after S phase due to targeted degradation.** A) Schematic of experimental procedure used to synchronize Eco1-3V5 cells. B) DNA content of cells showcasing cell cycle progression and synchronizations as outlined in (A). C) Detection of Eco1 protein levels (using anti-V5) by Western blot for the time course in (A). PGK detection is used as a loading control.

<https://doi.org/10.1371/journal.pone.0242968.g001>

Possible mechanisms for increased Eco1 protein include inhibiting either Eco1 phosphorylation (making Eco1 refractile to SCF-dependent degradation) or the SCF degradation machinery [34,36]. If either of these stabilization-based models is correct, then the rise of Eco1 protein levels that occur in response to DNA damage should persist in cells treated with the translation inhibitor cycloheximide (CHX). To test this prediction, log phase cells were synchronized in early S phase (HU), washed and then released into media supplemented with NZ (Fig 2A). The resulting pre-anaphase cells were then exposed, for 1hr, to either CHX, MMS or both MMS and CHX (Fig 2A). Log phase cell synchronizations in S and M phases were monitored by flow cytometry (Fig 2B). Pre-anaphase cells exposed to MMS for 1hr exhibited a two-fold increase in Eco1 protein levels, compared to cells not exposed to MMS (Fig 2C). Importantly, Eco1 protein levels were instead dramatically reduced in cells co-incubated with both MMS and CHX, compared to cells exposed to MMS alone (Fig 2C). Rad53 phosphorylation was detected in cells treated with MMS alone and also cells co-treated with MMS and CHX (Fig 2), indicating the efficacy of DNA damage induction in both treatments. These results challenge the prediction stated above and suggest instead that the degradation machinery is active and targeting Eco1 during M phase, even in the presence of DNA damage.

Given that Eco1 protein levels fail to increase in M phase cells co-incubated in MMS and CHX, we were concerned that CHX may deplete Eco1 protein levels before the DNA damage response inhibits Eco1 degradation. The fact that Eco1 protein levels remained low during CHX and MMS co-incubation further suggested that the degradation machinery was fully

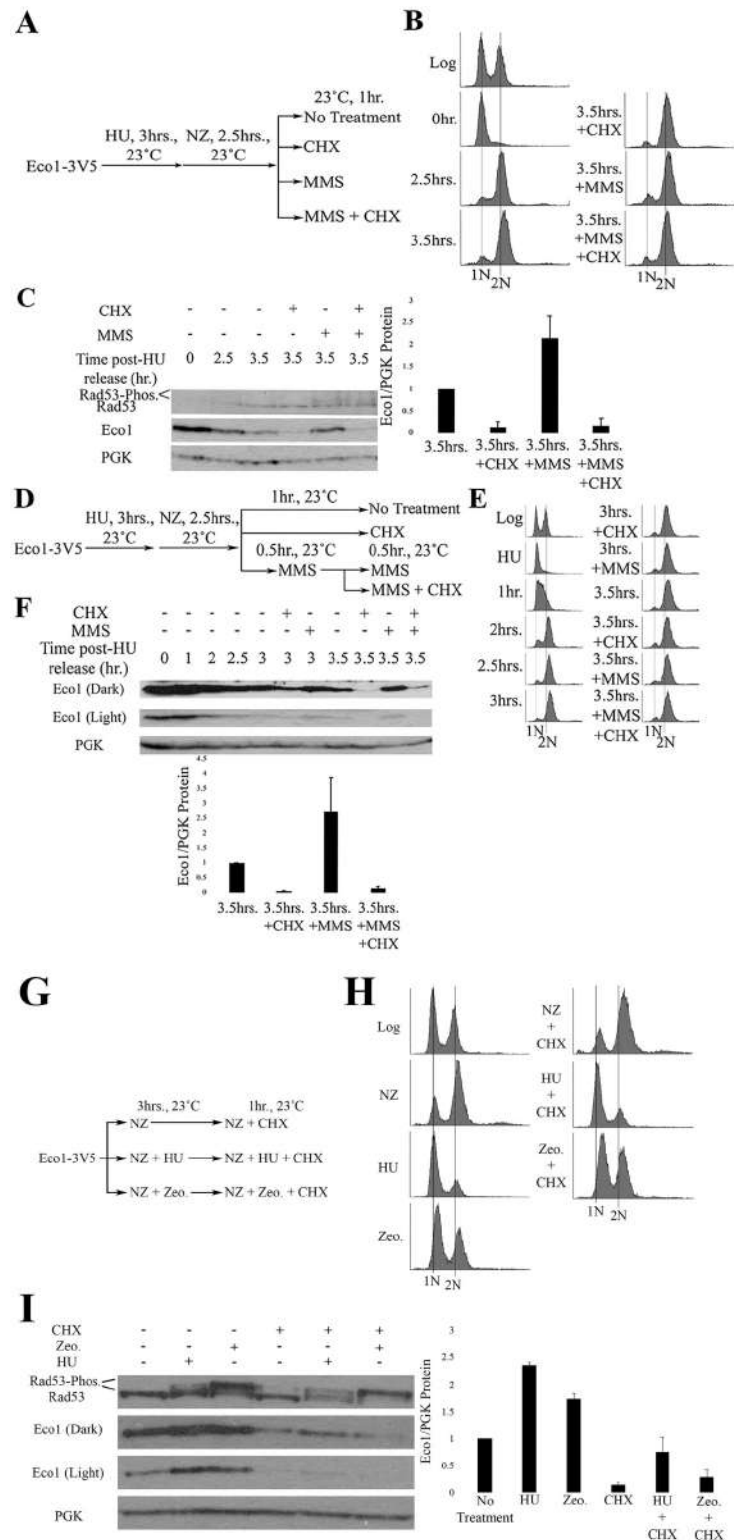


**Fig 2. DNA damage induces synthesis of new Eco1 protein.** A) Schematic of experimental procedure used to synchronize Eco1-3V5 cells and induce DNA damage during M phase. B) DNA content of Eco1-V5 cells showing cell cycle progression and synchronizations. C) Representative western blots (anti-V5) and quantification of Eco1 protein levels, normalized to PGK. Rad53 phosphorylation is provided as a positive control for the induction of DNA damage during M phase. For Eco1 quantifications, N = 3 for all samples at the 3.5hr timepoint. Error bars indicate

standard error of the mean. Statistical analysis was performed using a One-tail Student's T-test.  $p = 0.037$  for the 3.5hr samples, compared to 3.5hr+MMS samples. Statistical differences are based on  $p < 0.1$ . D) Schematic of experimental procedure used to synchronize Eco1-3V5 cells and induce damage during M phase, by pre-treating cells with MMS, followed by CHX treatment. E) DNA content of Eco1-V5 cells showcasing cell cycle progression and synchronizations. F) Eco1-V5 detection, by Western blot (anti-V5) and quantification for the time course shown in (D). For Eco1-V5 quantification,  $N = 3$  for all samples at the 3.5hr timepoint. Error bars indicate standard error of the mean. Statistical analysis was performed using a One-tail Student's T-test.  $p = 0.099$  for the 3.5hr, compared to 3.5hr+MMS samples. Statistical differences are based on  $p < 0.1$ . G) Schematic of experimental procedure used to synchronize Eco1-3V5 cells and induce DNA damage. H) DNA content of Eco1-3V5 cells showcasing cell cycle state and synchronizations. I) Representative western blots and quantification of Eco1 protein levels, normalized to PGK. Rad53 phosphorylation is provided as a positive control for the induction of DNA damage. For Eco1 quantifications,  $N = 2$  for HU and Zeocin samples.  $N = 3$  for NZ + CHX, HU + CHX and Zeocin + CHX samples. Errors bars indicate standard error of the mean. For induction of Eco1 in response to DNA damage, statistical analysis was performed using a One-tail Student's T-test.  $p = 0.028$  and  $0.087$  for induction of Eco1 in response to HU and Zeocin compared to untreated (NZ), respectively. Statistical differences are based on  $p < 0.1$ . For changes in Eco1 protein level in response to DNA damage and CHX treatment, statistical analysis was performed using a Two-tail Student's T-test.  $p = 0.045$  and  $0.143$  for HU + CHX and Zeocin + CHX compared to untreated (CHX). Statistical differences are based on  $p < 0.1$ .  $p = 0.066$  for HU + CHX compared to Zeocin + CHX. Statistical differences are based on  $p < 0.1$ .

<https://doi.org/10.1371/journal.pone.0242968.g002>

active, despite the presence of DNA damage. To test both of these models, we increased Eco1 protein (MMS) prior to CHX. Log phase cells were synchronized in early S phase (HU), washed, and released into fresh medium containing NZ to arrest cells in preanaphase (Fig 2D). Cell cycle progression was monitored using flow cytometry (Fig 2E). The resulting M phase cells were divided into three cultures, each of which contain NZ to maintain the pre-anaphase state (Fig 2D). The first culture was untreated for the remainder of the experiment—1 hour. The remaining two cultures were exposed to either CHX for 1 hour or MMS for 30 minutes (the latter to obtain elevated Eco1 protein levels) before subsequent addition of CHX for the remaining 30 minutes (Fig 2D). Replicates in which Eco1 protein levels at the 2.5hr time point were less than the 3.5hr time points, despite MMS addition, were excluded from further analyses. As expected, Eco1 protein levels increased 2.5 fold following 1 hour treatment of MMS (Fig 2F). Even a 30 minute exposure to MMS was sufficient to increase Eco1 protein levels 1.5 fold, compared to untreated samples. Subsequent addition of CHX to MMS-treated cells, however, resulted in a dramatic decrease in Eco1 protein levels (Fig 2F).

Eco1 protein levels remain stable in cells treated with CHX after pre-treatment with HU and Zeocin [34]. This observation raised the possibility that our results could be attributed to a drug-specific effect of MMS treatment. To address this possibility, we incubated log phase cells in NZ, HU + NZ or Zeocin + NZ for three hours followed by subsequent treatment with CHX for one hour (Fig 2G). Cell cycle state and Eco1 protein levels were monitored by flow cytometry and western blot, respectively (Fig 2H & 2I). Exposure to HU and Zeocin resulted in 2.4- and 1.8-fold increases in Eco1 protein levels, relative to cells treated with NZ alone (Fig 2I). Importantly, subsequent treatment with CHX for one hour significantly reduced Eco1 protein levels that were upregulated in response to either HU and Zeocin. Eco1 protein levels remained higher in HU-treated cultures compared to Zeocin-treated cultures (Fig 2I). Rad53 phosphorylation was detected in HU- and Zeocin-treated cells, indicating successful induction of the DNA damage response. In summary, these results reveal that 1) Eco1-targeting and degradation machinery is regulated not by the presence of DNA damage but by replication origin firing and 2) that DNA damage causes Eco1 levels to increase (possibly through a transcription-based mechanism) in a manner that significantly outpaces the rate of Eco1 turnover.

## DNA damage induces Eco1 transcription

Given that CHX negates the MMS-dependent increase in Eco1 protein levels, it became important to directly test whether the rate of either *ECO1* transcription or translation increases

in response to DNA damage. Mid-log phase cells were exposed for 1 hour to either genotoxic agents (MMS, Zeocin, or HU) alone or in combination with CHX (Fig 3A). Eco1 protein and mRNA levels were then quantified by Western blot and qRT-PCR, respectively. In the absence of CHX, individual treatments to either MMS, Zeocin or HU produced an approx. 2-fold increase in Eco1 protein; a response which trends toward statistical significance (Fig 3B). The addition of CHX, however, abolished induction of Eco1 protein levels in response to each of the DNA damaging agents (Fig 3B). We then tested whether the increase in Eco1 protein corresponded to increased mRNA levels. Results from qRT-PCR revealed a trend indicating increases in *ECO1* mRNA under all conditions of genotoxic stress, although these results were not statistically significant (Fig 3C; S1 Table). Thus, DNA damage increases *ECO1* expression to promote high fidelity DNA repair.

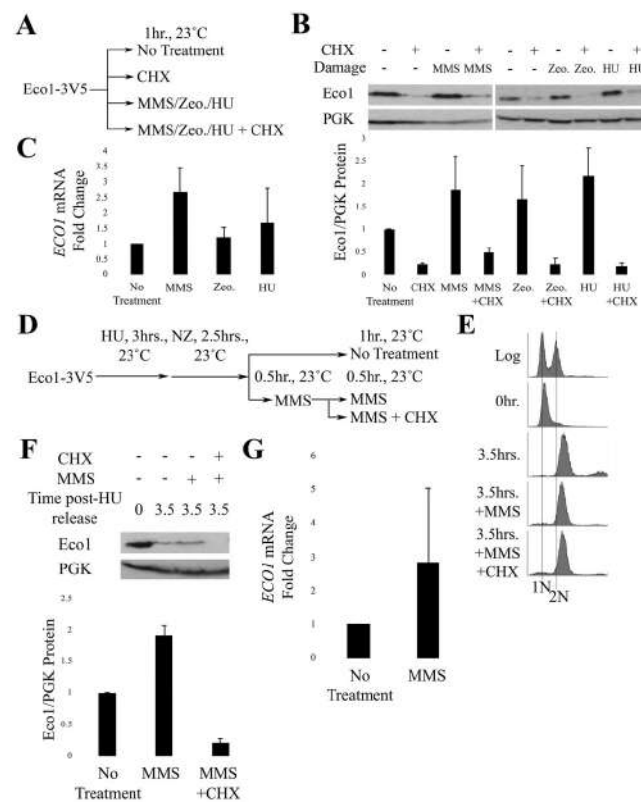


**Fig 3. DNA damage induces Eco1 transcription.** A) Schematic of experimental procedure. B) Representative western blot and quantification of Eco1-V5 cells for the experiment described in (A). For Eco1-V5 quantification, N = 2 for MMS-, Zeocin- and HU-treated samples. Error bars indicated standard error of the mean. Statistical analysis was performed using a One-tail Student's T-test.  $p = 0.117, 0.116, 0.099$  for the untreated compared to MMS-, Zeocin- and HU-treated samples, respectively. Statistical differences are based on  $p < 0.1$ . C) qRT-PCR data from the experiment in (A). Eco1 expression levels are shown for cells treated with MMS (N = 3), Zeocin (N = 3), or HU (N = 2). Error bars indicate standard error of the mean. Statistical analysis was performed using a One-tail Student's T-test.  $p = 0.052, 0.273, 0.313$  for cells treated with either MMS, Zeocin or HU, respectively, compared to untreated. Statistical differences are based on  $p < 0.1$ . D) Schematic of experimental procedure used to synchronize Eco1-3V5 cells and perform damage induction in M phase with MMS. E) DNA content of Eco1-V5 cells showcasing cell cycle progression and synchronizations for strategy shown in (D). F) Representative western blot and quantification of Eco1-V5 for the time course in (D). For Eco1-V5 protein level quantifications, N = 2 for all samples at the 3.5hr timepoint. Error bars indicate standard error of the mean. Statistical analysis was performed using a One-tail Student's T-test.  $p = 0.016$  for the 3.5hr, compared to 3.5hr+MMS samples. Statistical differences are based on  $p < 0.1$ . G) qRT-PCR data from the experiment shown in (D). Eco1 expression levels of cells treated with MMS only. Error bars indicate standard error of the mean. Statistical analysis was performed using a One-tail Student's T-test.  $p = 0.241$  for the untreated, compared to 3.5hr+MMS samples. Statistical differences are based on  $p < 0.1$ .

<https://doi.org/10.1371/journal.pone.0242968.g003>

DIC is an M-phase response to DNA damage, prompting us to test whether DNA damage-induced *ECO1* expression occurs specifically during M phase? To address this question, we modified the above experiment to arrest cells in preanaphase following release from an S phase synchronized culture (Fig 3D). The resulting pre-anaphase cells were divided into three cultures, the first untreated for 60 minutes. The second was incubated in medium containing MMS for 60 minutes, while the third was incubated in MMS for 30 minutes followed by co-incubation with MMS and CHX for an additional 30 minutes (Fig 3E). Western blot analyses of whole cell lysates reveal that Eco1 protein levels clearly rise during M phase in response to MMS (Fig 3F), but this increase is completely abolished by subsequent addition of CHX (Fig 3F). Importantly, qRT-PCR analysis revealed trends for increased *ECO1* mRNA levels in M-phase cells exposed to MMS, although these results were not statistically significant (Fig 3G; S2 Table). Taken together, these findings reveal that DNA damage induces *ECO1* transcription, even during M phase, at a level that exceeds that of Eco1 degradation.

### DNA damage-induced transcription of Eco1 is Yap5-dependent

Yap5 is an iron-sensitive and stress response transcription factor implicated in Eco1 regulation [48]. We hypothesized that the induction of *ECO1* transcription, in response to DNA damage, might occur through a Yap5-dependent mechanism. To test this hypothesis, we exploited a DNA damage induction experiment previously performed by Morgan and colleagues [34] (Fig 4A). Briefly, log phase *WT* and *yap5* cells were treated with either NZ or NZ and HU for 3hrs at 23°C in order to compare *ECO1* mRNA levels within one cell cycle between the two strains (Fig 4A). We also monitored changes in *RNR3* expression as a positive control [53]. As expected, *RNR3* mRNA levels increased dramatically in response to HU (S3 Table). *ECO1* mRNA levels also rose in response to HU (Fig 4B; S4 Table), consistent with our prior results. Importantly, *ECO1* mRNA levels were significantly repressed in *yap5* mutant cells, despite the presence of HU (Fig 4B; S4 Table). Taken together, these results suggest that Yap5 is necessary and sufficient for induction of *ECO1* transcription in response to DNA damage.

### Discussion

Mutations that occur through either endogenous or exogenous genotoxic agents contribute to both aging and diseases such as cancer. Cohesin is critical for DSB repair in a process that requires the acetyltransferase Eco1 [12,13,39,40,42]. The first major finding of the current study is elucidation of the mechanism through which Eco1 becomes reactivated during M phase and in response to DNA damage (Fig 5). Previous work revealed the central mechanism through which Eco1 activity is limited to S phase: sequential phosphorylations (Cdk1, DDK and Mck1 kinase) that promote ubiquitination (SCF E3 ligase) and subsequent degradation (proteasome) [34,36]. These findings formally raised the possibility that Eco1 reactivation during M might occur either by blocking Eco1 phosphorylation or degradation. Instead, our results reveal that DNA damage results in a significant increase in Eco1 protein levels despite continued Eco1 degradation. This increase is solely due to new synthesis, providing a transcriptional view of Eco1-dependent DNA repair (Fig 5).

How is Eco1 transcription regulated? Early work mapped Eco1 function specifically to S phase and that *ECO1* transcription peaks during S phase [5,54], but a mechanism for *ECO1* induction in response to DNA damage during M phase remained unknown. A second major finding of the current work is that Yap5 is critical for *ECO1* upregulation in response to DNA damage. Our findings extend the role of Yap5, a transcription factor that induces *ECO1* transcription in response to elevated iron levels [48], to include a DNA damage response. Both DNA damage and iron can generate reactive oxygen species (ROS). In turn, ROS triggers an

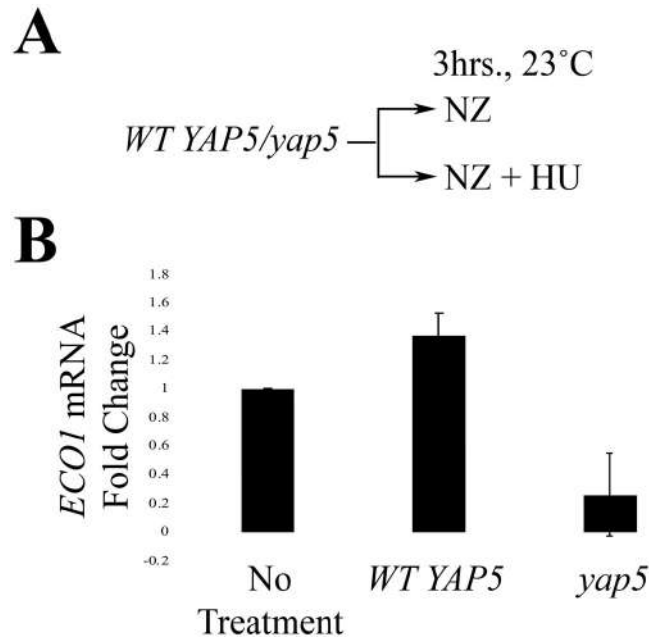


**Fig 4. DNA damage induces Yap5-dependent transcription of *ECO1*.** A) Schematic of experimental procedure used to synchronize *wildtype* and *yap5* mutant cells and induce DNA damage (HU). B) qRT-PCR data from the experiment strategy shown in (A) (N = 3). Error bars indicate standard error of the mean.  $p = 0.043$  for the untreated, compared to HU-treated samples in the WT strain (One-tail Student's T-test).  $p = 0.085$  for the untreated vs. HU-treated samples in the *yap5* strain (Two-tail Student's T-test).  $p = 0.005$  for WT vs. *yap5* (Two-tail Student's T-test). Statistical differences are based on  $p < 0.1$  for all tests.

<https://doi.org/10.1371/journal.pone.0242968.g004>

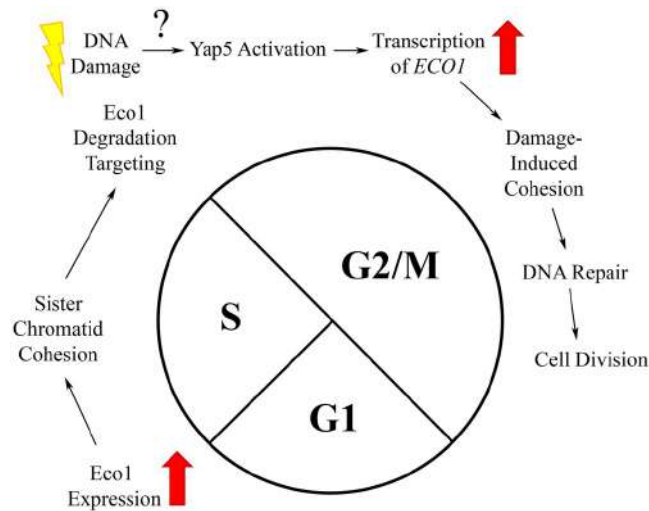


**Fig 5. Summary model of *Eco1* regulation in response to DNA damage.** In unperturbed cells, *ECO1* expression is upregulated at the G1/S transition, enabling sister chromatid cohesion establishment during S phase. Exit from S phase results in *Eco1* phosphorylation/ubiquitination and subsequent degradation—which persists through mitosis. In response to DNA damage during M phase, however, Yap5 induces new expression of *ECO1* at a rate that exceeds the rate of *Eco1* degradation.

<https://doi.org/10.1371/journal.pone.0242968.g005>

oxidative stress response that protects against macromolecular damage. This highlights cross-talk between the DNA repair and oxidative stress responses in which Yap5 likely plays a role [55–67]. Other transcription factors in the YAP family, most notably Yap1, have been implicated in both the yeast oxidative stress and DNA damage response pathways [60,63,65,68–72]. Intriguingly, Yap1 and Yap5 bind to the same consensus sequence in DNA and are proposed to overlap functionally [47]. Therefore, control of *ECO1* transcription might represent a unified and conserved pathway that evolved to promote redundancy in protecting the genome from a host of genotoxic agents.

The upregulation of *ECO1*, in response to DNA damage, has implications to human diseases and development. Roberts syndrome is currently modeled as a mitotic failure syndrome [73–77], although emerging evidence supports instead a major role in transcription dysregulation [78–80]. It is important to note in addition that both human and yeast models of RBS exhibit genotoxic sensitivity. We posit that defects in appropriate DNA damage responses, that include a failure to upregulate *ESCO2*, may constitute a critical but as yet unrecognized role in developmental defects [81–83]. The findings presented here demonstrate the complexity of cellular responses to DNA damage and provide tools for future endeavors that may further link *Eco1* function and expression in disease and development.

## Supporting information

**S1 Fig. *Eco1* protein levels are low in G1 phase, peak during S phase and decline in M phase due to targeted degradation.** A) Schematic of experimental procedure used to synchronize *Eco1*-3V5 cells. B) DNA content of cells showcasing cell cycle progression and synchronizations as outlined in (A). C) Detection of *Eco1* protein levels (using anti-V5) by Western blot for the time course in (A). PGK detection is used as a loading control.  
(TIF)

**S2 Fig. MMS-induced DNA damage induces *Eco1* upregulation in log phase and M phase-arrested cells.** A) Schematic of experimental procedure used to synchronize *Eco1*-3V5 cells and induce DNA damage. B) DNA content of *Eco1*-3V5 cells showcasing cell cycle progression and synchronizations. C) Representative western blots and quantification of *Eco1* protein levels, normalized to PGK. Rad53 phosphorylation is provided as a positive control for the induction of DNA damage. N = 2 for *Eco1* quantifications. Errors bars indicate standard error of the mean.  
(TIF)

**S1 Table. Raw qRT-PCR data for Fig 3C.**  
(DOCX)

**S2 Table. Raw qRT-PCR data for Fig 3G.**  
(DOCX)

**S3 Table. Raw qRT-PCR data for *RNR3* induction in response to HU.**  
(DOCX)

**S4 Table. Raw qRT-PCR data for Fig 4B.**  
(DOCX)

## Acknowledgments

We thank the Skibbens lab members (Donglai Shen, Caitlin Zuilkoski, Annie Sanchez and Nicole Kirven), Layden lab members (Michael Layden, Jamie Havrilak, Layla Al-Shaer and

Dylan Faltine-Gonzalez), Mary Kathryn Iovine and Shashwatti Bhattacharya for their helpful discussions throughout this process. We also thank the lab of Dr. Gregory Lang for sharing of reagents.

## Author Contributions

**Conceptualization:** Michael G. Mfarej, Robert V. Skibbens.

**Data curation:** Michael G. Mfarej.

**Formal analysis:** Michael G. Mfarej, Robert V. Skibbens.

**Funding acquisition:** Robert V. Skibbens.

**Investigation:** Michael G. Mfarej.

**Methodology:** Michael G. Mfarej, Robert V. Skibbens.

**Project administration:** Robert V. Skibbens.

**Supervision:** Robert V. Skibbens.

**Writing – original draft:** Michael G. Mfarej.

**Writing – review & editing:** Michael G. Mfarej, Robert V. Skibbens.

## References

1. Onn I, Heidinger-Pauli JM, Guacci V, Ünal E, Koshland DE. Sister Chromatid Cohesion: A Simple Concept with a Complex Reality. *Ann Rev Cell Dev Biol.* 2008; 24(1): 105–129. <https://doi.org/10.1146/annurev.cellbio.24.110707.175350> PMID: 18616427
2. Skibbens RV. Establishment of Sister Chromatid Cohesion. *Curr Biol.* 2009; 19(24): R1126–R1132. <https://doi.org/10.1016/j.cub.2009.10.067> PMID: 20064425
3. Nasmyth K, Haering CH. Cohesin: Its Roles and Mechanisms. *Ann Rev Genet.* 2009; 43(1): 525–558. <https://doi.org/10.1146/annurev-genet-102108-134233> PMID: 19886810
4. Uhlmann F. A matter of choice: The establishment of sister chromatid cohesion. *EMBO Rep.* 2009; 10(10): 1095–1102. <https://doi.org/10.1038/embor.2009.207> PMID: 19745840
5. Skibbens RV, Corson LB, Koshland D, Hieter P. Ctf7p is essential for sister chromatid cohesion and links mitotic chromosome structure to the DNA replication machinery. *Genes Dev.* 1999; 13(3): 307–319. <https://doi.org/10.1101/gad.13.3.307> PMID: 9990855
6. Toth A, Ciosk R, Uhlmann F, Galova M, Schleiffer A, Nasmyth K. Yeast Cohesin complex requires a conserved protein, Eco1p(Ctf7), to establish cohesion between sister chromatids during DNA replication. *Genes Dev.* 1999; 13(3): 320–333. <https://doi.org/10.1101/gad.13.3.320> PMID: 9990856
7. Ivanov D, Schleiffer A, Eisenhaber F, Mechtler K, Haering CH, Nasmyth K. Eco1 Is a Novel Acetyltransferase that Can Acetylate Protein Involved in Cohesion. *Curr Biol.* 2002; 4(19): 323–328. [https://doi.org/10.1016/s0960-9822\(02\)00681-4](https://doi.org/10.1016/s0960-9822(02)00681-4) PMID: 11864574
8. Lengronne A, McIntyre J, Katou Y, Kanoh Y, Hopfner K-P, Shirahige K, et al. Establishment of Sister Chromatid Cohesion at the *S. cerevisiae* Replication Fork. *Mol Cell.* 2006; 23(6): 787–799. <https://doi.org/10.1016/j.molcel.2006.08.018> PMID: 16962805
9. Ünal E, Heidinger-Pauli JM, Kim W, Guacci V, Onn I, Gygi SP, et al. A Molecular Determinant for the Establishment of Sister Chromatid Cohesion. *Science.* 2008; 321(5888): 566–569. <https://doi.org/10.1126/science.1157880> PMID: 18653894
10. Rolef Ben-Shahar T, Heeger S, Lehane C, East P, Flynn H, Skehel M, et al. Eco1-Dependent Cohesin Acetylation During Establishment of Sister Chromatid Cohesion. *Science.* 2008; 321(5888): 563–566. <https://doi.org/10.1126/science.1157774> PMID: 18653893
11. Spencer F, Gerring SL, Connelly C, Hieter P. Mitotic chromosome transmission fidelity mutants in *Saccharomyces cerevisiae*. *Genetics.* 1990; 124(2): 237–249. PMID: 2407610
12. Ström L, Karlsson C, Lindroos HB, Wedahl S, Katou Y, Shirahige K, et al. Postreplicative Formation of Cohesion Is Required for Repair and Induced by a Single DNA Break. *Science.* 2007; 317(5835): 242–245. <https://doi.org/10.1126/science.1140649> PMID: 17626884

13. Ünal E, Heidinger-Pauli JM, Koshland D. DNA Double-Strand Breaks Trigger Genome-Wide Sister-Chromatid Cohesion Through Eco1 (Ctf7). *Science*. 2007; 317(5835): 245–248. <https://doi.org/10.1126/science.1140637> PMID: 17626885
14. Guacci V, Koshland D. Cohesin-independent segregation of sister chromatids in budding yeast. *Mol Biol Cell*. 2012; 23(4): 729–739. <https://doi.org/10.1091/mbc.E11-08-0696> PMID: 22190734
15. Bellows AM, Kenna MA, Cassimeris L, Skibbens RV. Human EFO1p exhibits acetyltransferase activity and is a unique combination of linker histone and Ctf7p/Eco1p chromatid cohesion establishment domains. *Nucleic Acids Res*. 2003; 31(21): 6334–6343. <https://doi.org/10.1093/nar/gkg811> PMID: 14576321
16. Vega H, Waisfisz Q, Gordillo M, Sakai N, Yanagihara I, Yamada M, et al. Roberts syndrome is caused by mutations in ESCO2, a human homolog of yeast ECO1 that is essential for the establishment of sister chromatid cohesion. *Nat Genet*. 2005; 37(5): 468–470. <https://doi.org/10.1038/ng1548> PMID: 15821733
17. Hou F, Zou H. Two Human Orthologues of Eco1/Ctf7 Acetyltransferases Are Both Required for Proper Sister-Chromatid Cohesion. *Mol Biol Cell*. 2005; 16(8): 3908–3918. <https://doi.org/10.1091/mbc.e04-12-1063> PMID: 15958495
18. Ryu B, Kim DS, Deluca AM, Alani RM. Comprehensive Expression Profiling of Tumor Cell Lines Identifies Molecular Signatures of Melanoma Progression. *PLoS One*. 2007; 2(7): e594. <https://doi.org/10.1371/journal.pone.0000594> PMID: 17611626
19. Gordillo M, Vega H, Trainer AH, Hou F, Sakai N, Luque R, et al. The molecular mechanism underlying Roberts syndrome involves loss of ESCO2 acetyltransferase activity. *Hum Mol Genet*. 2008; 17(14): 2172–2180. <https://doi.org/10.1093/hmg/ddn116> PMID: 18411254
20. Luedeke M, Linnert CM, Hofer MD, Surowy HM, Rinckleb AE, Hoegel J, et al. Predisposition for TMPRSS2-ERG Fusion in Prostate Cancer by Variants in DNA Repair Genes. *Cancer Epidemiol Biomarkers Prev*. 2009; 18(11): 3030–3035. <https://doi.org/10.1158/1055-9965.EPI-09-0772> PMID: 19861517
21. Carson DR, Christman MF. Evidence that replication fork components catalyze establishment of cohesion between sister chromatids. *Proc Natl Acad Sci USA*. 2001; 98(15): 8270–8275. <https://doi.org/10.1073/pnas.131022798> PMID: 11459963
22. Kenna MA, Skibbens RV. Mechanical Link between Cohesion Establishment and DNA Replication: Ctf7p/Eco1p, a Cohesion Establishment Factor, Associates with Three Different Replication Factor C Complexes. *Mol Cell Biol*. 2003; 23(8): 2999–3007. <https://doi.org/10.1128/mcb.23.8.2999-3007.2003> PMID: 12665596
23. Moldovan G, Pfander B, Jentsch S. PCNA Controls Establishment of Sister Chromatid Cohesion during S Phase. *Mol Cell*. 2006; 23(5): 723–732. <https://doi.org/10.1016/j.molcel.2006.07.007> PMID: 16934511
24. Zhang J, Shi X, Li Y, Kim B-J, Jia J, Huang Z, et al. Acetylation of Smc3 by Eco1 Is Required for S Phase Sister Chromatid Cohesion in Both Human and Yeast. *Mol Cell*. 2008; 31(1): 143–151. <https://doi.org/10.1016/j.molcel.2008.06.006> PMID: 18614053
25. Maradeo ME, Skibbens RV. The Elg1-RFC Clamp-Loading Complex Performs a Role in Sister Chromatid Cohesion. *PLoS One*. 2009; 4(3): e4707. <https://doi.org/10.1371/journal.pone.0004707> PMID: 19262753
26. Maradeo ME, Skibbens RV. Replication Factor C Complexes Play Unique Pro- and Anti-Establishment Roles in Sister Chromatid Cohesion. *PLoS One*. 2010; 5(10): e153381. <https://doi.org/10.1371/journal.pone.0015381> PMID: 21060875
27. Maradeo ME, Garg A, Skibbens RV. Rfc5p regulates alternate RFC complex function in sister chromatid pairing reaction in budding yeast. *Cell Cycle*. 2010; 9(21): 4370–4378. <https://doi.org/10.4161/cc.9.21.13634> PMID: 20980821
28. Parnas O, Kupiec M. Establishment of sister chromatid cohesion: The role of the clamp loaders. *Cell Cycle*. 2010; 9(23): 4607–4615.
29. Zhang J, Shi D, Li X, Ding L, Tang J, Liu C, et al. Rtt101-Mms1-Mms22 coordinates replication-coupled sister chromatid cohesion and nucleosome assembly. *EMBO Rep*. 2017; 18: 1294–1305. <https://doi.org/10.15252/embr.201643807> PMID: 28615292
30. Zhang W, Yeung C, Wu L, Yuen WY. E3 ubiquitin ligase Bre1 couples sister chromatid cohesion establishment to DNA replication in *Saccharomyces cerevisiae*. *eLife*. 2017; 6: e28231. <https://doi.org/10.7554/eLife.28231> PMID: 29058668
31. Bender D, Da Silva EML, Chen J, Poss A, Gaway L, Rulon Z, et al. Multivalent interaction of ESCO2 with the replication machinery is required for sister chromatid cohesion in vertebrates. *Proc Natl Acad Sci USA*. 2020; 117(2): 1081–1089. <https://doi.org/10.1073/pnas.1911936117> PMID: 31879348

32. Bousset K, Diffley JFX. The cdc7 protein kinase is required for origin firing during S phase. *Genes Dev.* 1998; 12: 480–490. <https://doi.org/10.1101/gad.12.4.480> PMID: 9472017
33. Donaldson AD, Fangman WL, Brewer BJ. Cdc7 is required through the yeast S phase to activate replication origins. *Genes Dev.* 1998; 12: 491–501. <https://doi.org/10.1101/gad.12.4.491> PMID: 9472018
34. Lyons NA, Fonslow BR, Diedrich JK, Yates JR 3rd, Morgan DO. Sequential primed kinases create a damage-responsive phosphodegron on Eco1. *Nat Struct Mol Biol.* 2013; 20(2): 194–201. <https://doi.org/10.1038/nsmb.2478> PMID: 23314252
35. Seoane AI, Morgan DO. Firing of Replication Origins Frees Dbf4-Cdc7 to Target Eco1 for Destruction. *Curr Biol.* 2017; 27(18): 2849–2855. <https://doi.org/10.1016/j.cub.2017.07.070> PMID: 28918948
36. Lyons NA, Morgan DO. Cdk1-Dependent Destruction of Eco1 Prevents Cohesion Establishment after S Phase. *Mol Cell.* 2011; 42(3): 378–389. <https://doi.org/10.1016/j.molcel.2011.03.023> PMID: 21549314
37. Lafont AL, Song J, Rankin S. Sororin cooperates with the acetyltransferase Eco2 to ensure DNA replication-dependent sister chromatid cohesion. *Proc Natl Acad Sci USA.* 2010; 107(47): 20364–20369. <https://doi.org/10.1073/pnas.1011069107> PMID: 21059905
38. Minamino M, Tei S, Negishi L, Kanemaki MT, Yoshimura A, Sutani T, et al. Temporal Regulation of ESCO2 Degradation by the MCM Complex, the CUL4-DDB1-VPRBP Complex, and the Anaphase-Promoting Complex. *Curr Biol.* 2018; 28(16): 2665–2672. <https://doi.org/10.1016/j.cub.2018.06.037> PMID: 30100344
39. Ström L, Lindroos HB, Shirahige K, Sjögren C. Postreplicative Recruitment of Cohesin to Double-Strand Breaks Is Required for DNA Repair. *Mol Cell.* 2004; 16(6): 1003–1015. <https://doi.org/10.1016/j.molcel.2004.11.026> PMID: 15610742
40. Ünal E, Arbel-Eden A, Sattler U, Shroff R, Lichten M, Haber J, et al. DNA Damage Response Pathway Uses Histone Modification to Assemble a Double-Strand-Break Specific Cohesin Domain. *Mol Cell.* 2004; 16(6): 991–1002. <https://doi.org/10.1016/j.molcel.2004.11.027> PMID: 15610741
41. Heidinger-Pauli JM, Ünal E, Guacci V, Koshland D. The Kleisin Subunit of Cohesin Dictates Damage-Induced Cohesion. *Mol Cell.* 2008; 31(1): 47–56. <https://doi.org/10.1016/j.molcel.2008.06.005> PMID: 18614046
42. Heidinger-Pauli JM, Ünal E, Koshland D. Distinct Targets of the Eco1 Acetyltransferase Modulate Cohesion in S Phase and in Response to DNA Damage. *Mol Cell.* 2009; 34(3): 311–321. <https://doi.org/10.1016/j.molcel.2009.04.008> PMID: 19450529
43. Weinreich M, Stillman B. Cdc7p-Dbf4p kinase binds to chromatin during S phase and is regulated by both the APC and the Rad53 checkpoint pathway. *EMBO Rep.* 1999; 18: 5334–5346. <https://doi.org/10.1093/emboj/18.19.5334> PMID: 10508166
44. Takeda T, Ogino K, Tatebayashi K, Ikeda H, Arai K, Masai H. Regulation of Initiation of S phase, Replication Checkpoint Signaling and Maintenance of Mitotic Chromosome Structures during S phase by Hsk1 Kinase in the Fission Yeast. *Mol Biol Cell.* 2001; 12(5): 1257–1274. <https://doi.org/10.1091/mbc.12.5.1257> PMID: 11359920
45. Gabrielse C, Miller CT, McConnell KH, DeWard A, Fox CA, Weinreich M. A Dbf4p RCA1 C-Terminal-Like Domain Required for the Response to Replication Fork Arrest in Budding Yeast. *Genetics.* 2006; 173(2): 541–555. <https://doi.org/10.1534/genetics.106.057521> PMID: 16547092
46. Workman CT. A Systems Approach to Mapping DNA Damage Response Pathways. *Science.* 2006; 312(5776): 1054–1059. <https://doi.org/10.1126/science.1122088> PMID: 16709784
47. Tan K, Feizi H, Luo C, Fan SH, Ravasi T, Ideker TG. A systems approach to delineate functions of paralogous transcription factors: Role of the Yap1 family in the DNA damage response. *Proc Natl Acad Sci USA.* 2008; 105(8): 2934–2939. <https://doi.org/10.1073/pnas.0708670105> PMID: 18287073
48. Pimentel C, Vicente C, Menezes RA, Caetano S, Carreto L, Rodrigues-Pousada C. The Role of the Yap5 Transcription Factor in Remodeling Gene Expression in Response to Fe Bioavailability. *PLoS One.* 2012; 7(5): e37434. <https://doi.org/10.1371/journal.pone.0037434> PMID: 22616008
49. Tong K, Skibbens RV. Cohesin without Cohesion: A Novel Role for Pds5 in *Saccharomyces cerevisiae*. *PLoS One.* 2014; 9(6): e100470. <https://doi.org/10.1371/journal.pone.0100470> PMID: 24963665
50. Teste M, Duquenne, Francois JM, Parrou J. Validation of reference genes for quantitative expression analysis by real-time RT-PCR in *Saccharomyces cerevisiae*. *BMC Mol Biol.* 2009; 10: 99. <https://doi.org/10.1186/1471-2199-10-99> PMID: 19874630
51. Livak KJ, Schmittgen TD. Analysis of Relative Gene Expression Data Using Real-Time Quantitative PCR and the  $2^{-\Delta\Delta C_T}$  Method. *Methods.* 2001; 25(4): 402–408. <https://doi.org/10.1006/meth.2001.1262> PMID: 11846609
52. Schmittgen TD, Livak KJ. Analyzing real-time PCR data by the comparative  $C_T$  method. *Nat Protoc.* 2008; 3: 1101–1108. <https://doi.org/10.1038/nprot.2008.73> PMID: 18546601

53. Elledge JS, Davis RW. Two genes differentially regulated in the cell cycle and by DNA-damaging agents encode alternative regulatory subunits of ribonucleotide reductase. *Genes Dev.* 1990; 4: 740–751. <https://doi.org/10.1101/gad.4.5.740> PMID: 2199320
54. Spellman PT, Sherlock G, Zhang MQ, Iyer VR, Anders K, Eisen MB, et al. Comprehensive Identification of Cell Cycle-regulated Genes of the Yeast *Saccharomyces cerevisiae* by Microarray Hybridization. *Mol Bio Cell.* 1998; 9(12): 3273–3297. <https://doi.org/10.1091/mbc.9.12.3273> PMID: 9843569
55. Lindahl T. Instability and decay of the primary structure of DNA. *Nature.* 1993; 362(6422): 709–715. <https://doi.org/10.1038/362709a0> PMID: 8469282
56. Evert BA, Salmon TB, Song B, Jingjing L, Siede W, Doetsch PW. Spontaneous DNA Damage in *Saccharomyces cerevisiae* Elicits Phenotypic Properties Similar to Cancer Cells. *J Biol Chem.* 2004; 279(21): 22585–22594. <https://doi.org/10.1074/jbc.M400468200> PMID: 15020594
57. Salmon TB. Biological consequences of oxidative stress-induced DNA damage in *Saccharomyces cerevisiae*. *Nucleic Acids Res.* 2004; 32(12): 3712–3723. <https://doi.org/10.1093/nar/gkh696> PMID: 15254273
58. Carter CD, Kitchen LE, Au W, Babic CM, Basrai MA. Loss of SOD1 and LYS7 Sensitizes *Saccharomyces cerevisiae* to Hydroxyurea and DNA Damage Agents and Downregulates MEC1 Pathway Effectors. *Mol Cell Biol.* 2005; 25(23): 10273–10285. <https://doi.org/10.1128/MCB.25.23.10273-10285.2005> PMID: 16287844
59. Ragu S, Faye G, Iraqui I, Masurel-Heneman A, Kolodner RD, Huang ME. Oxygen metabolism and reactive oxygen species cause chromosomal rearrangements and cell death. *Proc Natl Acad Sci USA.* 2007; 104(23): 9747–9752. <https://doi.org/10.1073/pnas.0703192104> PMID: 17535927
60. Rowe LA, Degtyareva N, Doetsch PW. DNA damage-induced reactive oxygen species (ROS) stress response in *Saccharomyces cerevisiae*. *Free Radic Biol Med.* 2008; 45(8): 1167–1177. <https://doi.org/10.1016/j.freeradbiomed.2008.07.018> PMID: 18708137
61. Guo Z, Deshpande R, Paull TT. ATM activation in the presence of oxidative stress. *Cell Cycle.* 2010; 9(24): 4805–4811. <https://doi.org/10.4161/cc.9.24.14323> PMID: 21150274
62. Guo Z, Kozlov S, Lavin MF, Person MD, Paull TT. ATM Activation by Oxidative Stress. *Science.* 2010; 330(6003): 517–521. <https://doi.org/10.1126/science.1192912> PMID: 20966255
63. Rowe LA, Degtyareva N, Doetsch PW. Yap1: A DNA damage responder in *Saccharomyces cerevisiae*. *Mech Ageing Dev.* 2012; 133(4): 147–156. <https://doi.org/10.1016/j.mad.2012.03.009> PMID: 22433435
64. Yan S, Sorrell M, Berman Z. Functional interplay between ATM/ATR-mediated DNA damage response and DNA repair pathways in oxidative stress. *Cell Mol Life Sci.* 2014; 71(20): 3951–3967. <https://doi.org/10.1007/s00018-014-1666-4> PMID: 24947324
65. Yi DG, Kim MJ, Choi JE, Lee J, Jung J, Huh WK, et al. Yap1 and Skn7 genetically interact with Rad51 in response to oxidative stress and DNA double-strand break in *Saccharomyces cerevisiae*. *Free Radic Biol Med.* 2016; 101: 424–433. <https://doi.org/10.1016/j.freeradbiomed.2016.11.005> PMID: 27838435
66. Choi JE, Heo S, Kim MJ, Chung W. Lack of superoxide dismutase in a rad51 mutant exacerbates genomic instability and oxidative stress-mediated cytotoxicity in *Saccharomyces cerevisiae*. *Free Radic Biol Med.* 2018; 129: 97–106. <https://doi.org/10.1016/j.freeradbiomed.2018.09.015> PMID: 30223018
67. Choi JE, Chung W. Synthetic lethal interaction between oxidative stress response and DNA damage repair in the budding yeast and its application to targeted anticancer therapy. *J Microbiol.* 2018; 57(1): 9–17. <https://doi.org/10.1007/s12275-019-8475-2> PMID: 30594981
68. Moyer-Rowley WS, Harshman KD, Parker CS. Yeast YAP1 encodes a novel form of the jun family of transcriptional activator proteins. *Genes Dev.* 1989; 3: 283–292. <https://doi.org/10.1101/gad.3.3.283> PMID: 2542125
69. Coleman ST, Epping EA, Steggerda SW, Moyer-Rowley WS. Yap1p Activates Gene Transcription in an Oxidant-Specific Fashion. *Mol Cell Biol.* 1999; 19(12): 8302–8313. <https://doi.org/10.1128/mcb.19.12.8302> PMID: 10567555
70. Delaunay A, Isnard A, Toledano MB. H<sub>2</sub>O<sub>2</sub> sensing through oxidation of the Yap1 transcription factor. *EMBO J.* 2000; 19: 5157–5166. <https://doi.org/10.1093/emboj/19.19.5157> PMID: 11013218
71. Delaunay A, Pflieger D, Barrault M, Vinh J, Toledano M. A Thiol Peroxidase Is an H<sub>2</sub>O<sub>2</sub> Receptor and Redox-Transducer in Gene Activation. *Cell.* 2002; 111(4): 471–481. [https://doi.org/10.1016/s0092-8674\(02\)01048-6](https://doi.org/10.1016/s0092-8674(02)01048-6) PMID: 12437921
72. Rodrigues-Pousada CA, Nevitt T, Menezes R, Azevedo D, Pereira J, Amaral C. Yeast activator protein and stress response: an overview. *FEBS Lett.* 2004; 567(1): 80–85. <https://doi.org/10.1016/j.febslet.2004.03.119> PMID: 15165897
73. Morita A, Nakahira K, Hasegawa K, Uchida K, Taniguchi Y, Takeda S, et al. Establishment and characterization of Roberts syndrome and SC phocomelia model medaka. *Dev. Growth Differ.* 2012; 54(5): 588–604. <https://doi.org/10.1111/j.1440-169X.2012.01362.x> PMID: 22694322

74. Percival SM, Thomas HR, Amsterdam A, Carroll AJ, Lees JA, Yost HJ, et al. Variations in dysfunction of sister chromatid cohesion in *esco2* mutant zebrafish reflect the phenotypic diversity of Roberts syndrome. *Dis Model Mech*. 2015; 8: 941–955. <https://doi.org/10.1242/dmm.019059> PMID: 26044958
75. Afifi HH, Abdel-Salam G, Eid MM, Tossou A, Shousha W, Azeem A, et al. Expanding the mutation and clinical spectrum of Roberts syndrome. *Congenit Anom (Kyoto)*. 2016; 56(4): 154–162. <https://doi.org/10.1111/cga.12151> PMID: 26710928
76. Zhou J, Yang X, Jin X, Jia Z, Lu H, Qi Z, et al. Long-term survival after corrective surgeries in two patients with severe deformities due to Roberts syndrome: A case report and review of the literature. *Exp Ther Med*. 2018; 15(2): 1702–1711. <https://doi.org/10.3892/etm.2017.5592> PMID: 29434756
77. Columbo EA, Mutlu-Albayrak H, Shafeghati Y, Balasar M, Piard J, Genilini D, et al. Phenotypic Overlap of Roberts Syndromes in Two Patients With Craniosynostosis, Limb Reduction and *ESCO2* Mutations. *Front Pediatr*. 2019; 7: 2010.
78. Banerji R, Eble DM, Iovine MK, Skibbens RV. *Esco2* regulates *cx43* during skeletal regeneration in the zebrafish fin. *Dev Dyn*. 2016; 245(1): 7–21. <https://doi.org/10.1002/dvdy.24354> PMID: 26434741
79. Banerji R, Skibbens RV, Iovine MK. Cohesin mediates *Esco2*-dependent transcriptional regulation in a zebrafish regenerating fin model of Roberts Syndrome. *Biol Open*. 2017; 6: 1802–1813. <https://doi.org/10.1242/bio.026013> PMID: 29084713
80. Banerji R, Skibbens RV, Iovine MK. How many roads lead to cohesinopathies. *Dev Dyn*. 2017; 246(11): 881–888. <https://doi.org/10.1002/dvdy.24510> PMID: 28422453
81. van der Lelij P, Godthelp BC, van Zon W, van Gosliga D, Oostra AB, Steltenpool J, et al. The Cellular Phenotype of Roberts Syndrome Fibroblasts as Revealed by Ectopic Expression of *ESCO2*. *PLoS One*. 2009; 4(9): e6936. <https://doi.org/10.1371/journal.pone.0006936> PMID: 19738907
82. Lu S, Goering M, Gard S, Xiong B, McNairn AJ, Jaspersen SL, et al. *Eco1* is important for DNA damage repair in *S. cerevisiae*. *Cell Cycle*. 2010; 9(16): 3335–3347. <https://doi.org/10.4161/cc.9.16.12673> PMID: 20703090
83. McKay MJ, Craig J, Kalitsis P, Kozlov S, Verschoor S, et al. A Roberts Syndrome Individual With Differential Genotoxin Sensitivity and a DNA Damage Response Defect. *Int J Radiat Oncol Biol Phys*. 2019; 103(5): 1194–1202. <https://doi.org/10.1016/j.ijrobp.2018.11.047> PMID: 30508616